RSC Advances

COMMUNICATION

View Article Online
View Journal | View Issue

Cite this: *RSC Adv.*, 2015, **5**, 3508

Received 30th September 2014
Accepted 2nd December 2014

DOI: 10.1039/c4ra11526k

www.rsc.org/advances

Highly sensitive and colorimetric detection of hydrogen sulphide by *in situ* formation of Ag_2S@Ag nanoparticles in polyelectrolyte multilayer film†

Hongxia Fu and Xinrui Duan*

Ag_2S nanoparticles (NPs) were formed by reacting Ag^+ ions with H_2S gas in a polyelectrolyte multilayer film. Ag_2S NPs later catalyse the formation of Ag NPs. H_2S (when as low as 10 nM Na_2S was used as a donor) was sensitively detected by monitoring the UV-vis absorbance of the newly formed Ag NPs.

H_2S was discovered to be a gasotransmitter, along with nitric oxide and carbon monoxide.[1] H_2S influences cellular events through regulation of intracellular redox homeostasis and post-translational modification of proteins through S-sulfhydration.[2] H_2S can be endogenously generated by cystathionine beta-synthase (CBS), cystathionine gamma-lyase (CSE), and 3-mercaptopyruvate sulfurtransferase during cysteine metabolism. H_2S is mainly produced by CSE in the cardiovascular system, liver, kidney, and pancreas. More importantly, the H_2S level is related to Down's syndrome and Alzheimer's disease.[3]

Many methods have been developed for H_2S detection, including colorimetry,[4] a fluorescence technique,[5] electrochemical assays,[6] gas chromatography,[7] and nanofibers/wires and nanotube based methods.[8] A recent report has shown that hydrogen sulphide concentrations are much lower than presently accepted values in blood and tissues (100 pM in blood and 15 nM in tissues, respectively);[7] to our best knowledge, only polarography and gas chromatography-based methods have the ability to detect it, which requires the involvement of highly toxic mercury and/or complicated instruments. Recent advances of developing fluorescent probes and a colorimetry assay[9] have highlighted the need to develop a sensitive, selective, and rapid method for H_2S detection for disease diagnosis and *in vitro* cultured cell-based inhibitor screening for H_2S-related enzymes. To date, the lack of an affordable and sensitive method is still the major obstacle for such applications.

In this work, we would like to develop a sensitive, selective, and rapid method for H_2S detection based on Ag_2S NP catalysed formation of Ag NPs in a layer-by-layer polyelectrolyte multilayer film. Ag_2S NPs have previously been employed in colorimetric H_2S sensing.[4b] With a common microplate reader, the limit of detection is 8.7 μM. Formation of Ag_2S on a metallic silver probe caused a light reflection difference enabling concentrations as low as 100 nM of H_2S to be detected.[4c] By using Au@Ag NPs and sophisticated dark-field microscopy, H_2S as low as 50 nM could be detected.[4d]

Su and co-workers extensively studied the *in situ* formation of Ag NPs in layer-by layer polyelectrolyte multilayer films (PEMs).[10] Shannon and his co-workers have prepared Au/CuI and Au/CdS core–shell nanoparticles in poly (diallyl dimethylammonium) (PDDA) by using electrochemical atomic layer deposition.[11] Li and his co-workers have prepared CuS NPs in a PVA polymer matrix by embedding copper ions with H_2S gas.[12] Under the inspiration of these previous works and the fact that PEMs are very stable in aqueous solution, we designed our system as follows.

As shown in Scheme 1, PEMs were prepared by a standard layer-by-layer process in the presence of extra sodium ions. Sodium ions were later exchanged with Ag ions. At physiological pH, the assay takes advantage of the volatility of H_2S gas. As H_2S

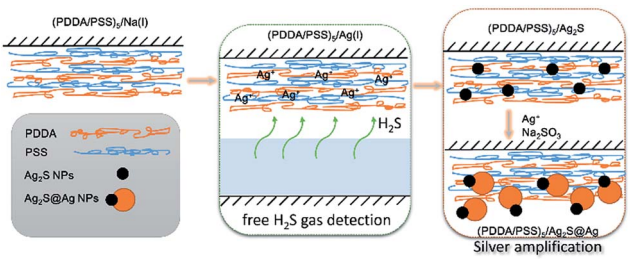

Scheme 1 Mechanism of H_2S gas detection.

Key Laboratory of Analytical Chemistry for Life Science of Shaanxi Province, School of Chemistry and Chemical Engineering, Shaanxi Normal University, Xi'an, Shaanxi, 710119, P. R. China. E-mail: duanxr@snnu.edu.cn

† Electronic supplementary information (ESI) available: Experimental details and UV-vis spectra of $(PDDA/PSS)_5/Ag_2S$ formed under a high concentration of Na_2S, effect of silver amplification time, spectra from EDX analysis. See DOI: 10.1039/c4ra11526k

is volatilized in a microplate well, it can react with the Ag ions to form Ag_2S NPs. Ag NPs can be generated on Ag_2S NPs by reducing Ag^+ ions with hydroquinone or sodium sulphite in solution.[13] UV light irradiation substantially accelerates this process. Because of this catalytic effect of Ag_2S NPs, Ag NPs were formed at Ag_2S NP sites in the PEMs in the presence of silver nitrate and Na_2SO_3, which greatly improved the sensitivity of detection. The concentrations of silver nitrate and sodium sulphite, and time of amplification have a great impact on the silver amplification process, thus we chose the previously reported optimized concentrations for our study. Furthermore, we optimized the time of amplification (Fig. S2†). Two hours of amplification produced the best signal/noise ratio.

We used Na_2S as the H_2S donor to develop our detection method, since the purity (>98%) is much higher than commercially available NaSH, which may contain polysulfides and have a purity of only 60%.[14] H_2S gas is spontaneously released from Na_2S aqueous solution until the HS– and S^{2-} are used up. H_2S reacted with the Ag ions embedded in the $(PDDA/PSS)_5$ film coated on the glass slide. After reaction with H_2S gas from the Na_2S solution, Ag_2S NPs formed in the nano-size spaces of the PEMs.[10a] Scanning electron microscopy (SEM) images and the absorption spectra of $(PDDA/PSS)_5/Ag^+$, $(PDDA/PSS)_5/Ag_2S$ and $(PDDA/PSS)_5/Ag_2S$@Ag PEMs are shown in Fig. 1. The magnification of all SEM images is 50 000×, except the inset image of Fig. 1b which is 100 000×. The $(PDDA/PSS)_5/Ag^+$ film does not have any significant morphology under SEM and has a weak absorption in the corresponding wavelength region due to absorption of glass.

Although the formed Ag_2S NPs can barely be seen under SEM, we could observe a roughness increase of the $(PDDA/PSS)_5/Ag_2S$ film (Fig. 1c). It produces a broad absorption band in UV-vis spectra (Fig. S1,† UV-vis spectra of highly concentrated Ag_2S NPs). Although SEM is not the ideal tool for characterization of Ag_2S NP morphology, the existence of silver NPs after silver amplification also supports the existence of earlier formed Ag_2S NPs. Ag amplification has been extensively studied where silver ions were reduced to metallic silver in the presence of a reducing agent (such as Na_2SO_3).[13] Previous work reported the catalytic effect of Ag_2S NPs in solution; in our work we also observed this phenomenon in the PEM films. After the silver amplification process, Ag NPs appear clearly under SEM (Fig. 1b). As for the UV-vis detection in Fig. 1d, a much stronger absorption peak appears around 430 nm after silver amplification. The inset image is an image of PEM films taken by a cell phone camera, which were on top of the PBS solution or the Na_2S solution in a 96 well plate after silver amplification. We can see the circular shapes of spots that well preserve the shape of wells. By converting the absorption signal of Ag_2S NPs to that of Ag NPs in the PEMs, the sensitivity of H_2S detection was greatly improved due to the following reasons: (1) the maximum absorption peak of Ag NPs is higher than 300 nm, which avoids the interference of the glass slide and cell culture plate itself; (2) the Ag_2S NPs serve as a catalyst, which results in significant signal amplification.

To get a direct view of the morphology and the composition of the Ag_2S@Ag NPs in the PEM films, we studied a sample with field emission transmission electron microscopy (FE-TEM) under a scanning TEM (STEM) mode and energy dispersive X-ray analysis (EDX) under STEM of single particles in a PEM film. The results are shown in Fig. 2. Since the NPs are crowded in high concentration samples (as shown in Fig. 1b), we chose a sample from a lower concentration of H_2S (500 nM) for all the STEM studies. The PEM film was prepared by scratching it off from the glass surface in water. The film floated on the water surface and later was caught by a TEM copper grid.

Fig. 2a shows the morphology of single NPs under FE-TEM by using a STEM mode. The size distribution of the NPs is shown in Fig. 2b. The majority of particles have a diameter between 20 and 70 nm. It is worth noticing, beside large and bright particles, some very small particles with the diameter of several nanometers can be seen surrounding bigger particles. This is more clearly visible with the higher magnification image in Fig. 2c. We assume that the smaller particles are Ag_2S NPs and that the bigger particles are Ag NPs which are newly formed on the Ag_2S NP sites. We did the line scan of STEM-EDX analysis to find out the content difference between the two types of particles. As shown in Fig. 2c, the net intensity of silver content is much higher than sulphur content on the bigger NPs. Since the intensity of a single small particle is too weak, we performed area analysis on a crowded area of small particles to get more comparable results with a spot from a bigger particle. The selection of the area and the spot are shown in Fig. 2d. Normalized atomic percentage and net intensities are shown in Fig. 2e and f, respectively. The atomic ratio of silver to sulphur in the 20 nm particle is around 3.2 : 1, which confirmed the formation of Ag_2S@Ag NPs. The atomic ratio of particles with the diameter of several nanometers is around 1.5, which is very

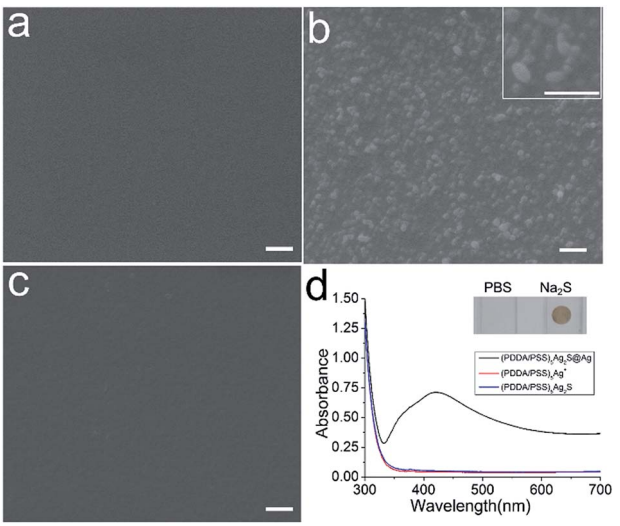

Fig. 1 SEM images of (a) $(PDDA/PSS)_5/Ag(I)$, (b) $(PDDA/PSS)_5/Ag_2S$@Ag, and (c) $(PDDA/PSS)_5/Ag_2S$. (d) UV-vis spectra of all films and inset is the image of PEM films on top of PBS solution or Na_2S solution after silver amplification. 10 μM Na_2S solution was used to generate all PEM films for SEM imaging and UV-vis spectra. The magnification of all SEM images is 50 000×, except the inset image of (b) which is 100 000×. Scale bar = 500 nm.

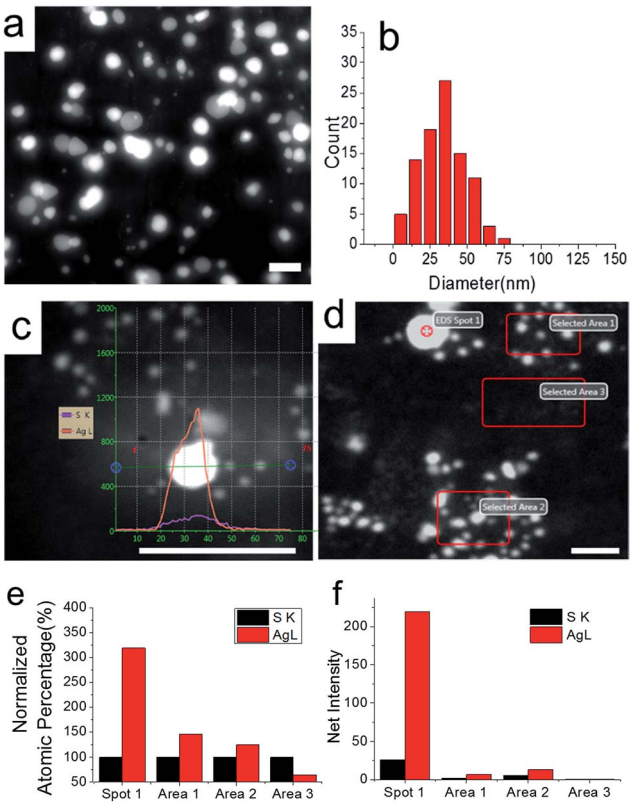

Fig. 2 (a) STEM image of NPs. (b) Size distribution of NPs. (c) Line scan of STEM-EDX analysis of silver and sulphur content of a single NP. (d) Spot and area analysis of silver and sulphur content by STEM-EDX. Scale bar = 100 nm. A 500 nM Na_2S solution was used to generate the PEM film for STEM imaging and EDX analysis.

close to the theoretical ratio of Ag_2S. This difference of ratio between our observed and theoretical ratios might be due to the low net intensities of area 1 and area 2, which will cause the increase of error. Area 3 was selected to show the background signals; from Fig. 2f, we can see that the background signals are negligible. Spectra from the EDX analysis are presented in Fig. S3.†

Fig. 3 shows a standard curve of various concentrations (from 10 nM to 5 μM) of Na_2S solutions *vs.* Ag_2S@Ag NP absorbance. A good linear relationship between the UV absorption at 430 nm and the concentration of Na_2S solution (10 nM–5 μM) was observed. The linearity equation is $A = 0.03928 + 4.03196C$. The R square value is 0.9980.

To test the specificity of our method, various biologically relevant molecules which include reactive sulfur such as dithiothreitol (DTT), cysteine (CYS), and reduced glutathione (GSH), as well as the cell culture medium DMEM and DMEM plus 10% fetal bovine serum (FBS) were studied. As shown in Fig. 4a, under the same reaction conditions, all interference candidates with a 2000-fold higher concentration of Na_2S only produce the same UV absorption intensity as the control (PBS buffer solution). These results demonstrate excellent selectivity of our method for H_2S gas detection. This high selectivity of our method is similar to previous reported hydrogen sulphide gas-based detection methods,[4b,5d] in which interference candidates only produce comparable signals to the control solutions.

With the excellent sensitivity and selectivity of our method, we were confident to perform the detection of cellular endogenous H_2S gas. Since H_2S is mainly produced by CSE in the liver, cardiovascular system, kidney and pancreas, the liver cancer cell line HepG2 was used in this section of the study. Detection cells were pre-treated with cysteine (CYS) and pyridoxal phosphate (PLP) to generate H_2S gas. Blanks, which underwent the same treatment without cells, were also included in the study. The CSE inhibitor propargylglycine (PAG) was added to test the inhibitor monitoring ability of our method in live cells.[3] PEM-coated glass slides were glued on to a 96 well plate cover and placed on top of a well plate for 2 hours, and after 2 hours the silver amplification process in the glass slides was measured using a microplate reader. As shown in Fig. 4b, 1×10^4 (10k) cells (*i.e.* about 30% coverage of a 0.32 cm^2 area) can be detected in a 96 well plate format, and 2×10^4 (20k) cells produce a higher signal than 10k cells. Since we used the same amount of PAG, absorbance of the sample of 20k cells to which PAG had been added also lightly increased. The signals from cells were

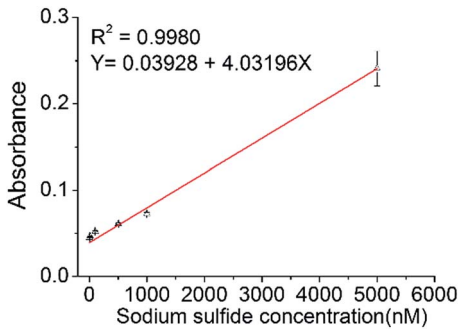

Fig. 3 Standard curve of H_2S detection (from 10 nM to 5000 nM), determined by measuring the absorbance of $(PDDA/PSS)_5/Ag_2S$@Ag. Error bars represent the standard deviations ($n = 3$). H_2S gas from Na_2S solution was used to react with $(PDDA/PSS)_5/Ag^+$ to generate $(PDDA/PSS)_5/Ag_2S$, which was further treated with a mixture of $AgNO_3$ and Na_2SO_3 solutions to generate $(PDDA/PSS)_5/Ag_2S$@Ag.

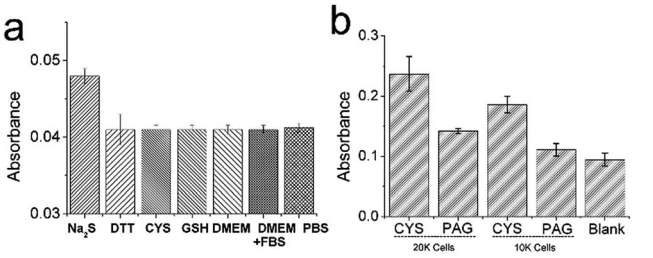

Fig. 4 (a) The effect of possible interference by DTT, CYS, GSH, DMEM, and DMEM plus 10% FBS on H_2S detection. A PBS solution was used as a control. The concentrations of these substances were all 200 μM, except Na_2S which was 100 nM. Error bars represent the standard deviations ($n = 3$). (b) Measurement of free H_2S gas generated from live HepG2 cells. Error bars represent the standard deviations ($n = 3$).

significantly higher than those from blank and PAG-treated samples.

A previous report on free H_2S gas detection of live cells is based on zinc salts embedded in an agar hydrogel.[5a] After 12 hours or longer incubation, acid was added to release H_2S gas from the formed ZnS precipitation, and the released H_2S gas reacted with *N*,*N*-dimethyl-*p*-phenylenediamine chloride and $FeCl_3$ to produce methylene blue. Measuring the absorbance of the produced methylene blue gave the quantity of H_2S gas. Our method holds two significant improvements: (1) the high sensitivity of our method shortens the incubation time from 12 hours to 2 hours; (2) *in situ* formation and silver amplification ensured that reacted spots were well preserved, so results can be readily obtained by using a micro-plate reader.

Conclusions

We reported a sensitive, selective, and rapid colorimetric method for cellular endogenous H_2S gas detection based on *in situ* formation of Ag_2S@Ag NPs in layer-by-layer PEMs. When using Na_2S solution as the gas source, H_2S from 10 nM (3 picomole, calculated by the sulfur) of 300 μL Na_2S solution in pH 7.0 buffer solution can be detected effectively. As far as we know, this method is the most sensitive among colorimetric methods and has comparable sensitivity with the most sensitive polarographic and gas chromatographic approaches. Furthermore, our method only required a microplate reader with UV-vis absorbance detecting ability for detection. The reaction between H_2S and silver ions generated Ag_2S NPs, which catalysed the rapid formation of Ag NPs on the Ag_2S NP surfaces, thus the absorption intensity of Ag_2S NPs was transferred to the absorbance of newly-formed Ag NPs. This results in signal amplification and high sensitivity. Since our method was designed to only measure H_2S gas, potential interferents including common thiols and standard DMEM medium plus 10% FBS do not affect detection. Due to its excellent sensitivity and selectivity, we believe our method is significantly important for disease diagnosis and *in vitro* cultured cell-based inhibitor screening for H_2S-related enzymes.

Acknowledgements

We thank the National Natural Science Foundation of China (Grant no. 21305083) and Fundamental Research Funds for the Central Universities (Grant no. GK201303003 and GK201402051) for financial support.

Notes and references

1 R. Wang, *Curr. Opin. Nephrol. Hypertens.*, 2011, **20**, 107–112.
2 (*a*) J. Pan and K. S. Carroll, *Biopolymers*, 2013, **101**, 165–172; (*b*) J. Yang, V. Gupta, K. S. Carroll and D. C. Liebler, *Nat. Commun.*, 2014, **5**, 4776.
3 (*a*) M. Thorson, T. Majtan, J. Kraus and A. Barrios, *Angew. Chem., Int. Ed.*, 2013, **52**, 4641–4644; (*b*) H. Peng, Y. Cheng, C. Dai, A. King, B. Predmore, D. Lefer and B. Wang, *Angew. Chem., Int. Ed.*, 2011, **50**, 9672–9675.
4 (*a*) R. Kartha, J. Zhou, L. Hovde, B. Cheung and H. Schröder, *Anal. Biochem.*, 2012, **423**, 102–108; (*b*) A. Jarosz, T. Yep and B. Mutus, *Anal. Chem.*, 2013, **85**, 3638–3643; (*c*) H. Kong, Z. Ma, S. Wang, X. Gong, S. Zhang and X. Zhang, *Anal. Chem.*, 2014, **86**, 7734–7739; (*d*) J. Hao, B. Xiong, X. Cheng, Y. He and E. Yeung, *Anal. Chem.*, 2014, **86**, 4663–4667.
5 (*a*) Y. Qian, J. Karpus, O. Kabil, S. Y. Zhang, H. L. Zhu, R. Banerjee, J. Zhao and C. He, *Nat. Commun.*, 2011, **2**, 495; (*b*) A. R. Lippert, E. J. New and C. J. Chang, *J. Am. Chem. Soc.*, 2011, **133**, 10078–10080; (*c*) Y. Chen, C. Zhu, Z. Yang, J. Chen, Y. He, Y. Jiao, W. He, L. Qiu, J. Cen and Z. Guo, *Angew. Chem., Int. Ed.*, 2013, **52**, 1688–1691; (*d*) A. Faccenda, J. Wang and B. Mutus, *Anal. Chem.*, 2012, **84**, 5243–5249; (*e*) Y. Zhou, J. Yu, X. Lei, J. Wu, Q. Niu, Y. Zhang, H. Liu, P. Christen, H. Gehring and F. Wu, *Chem. Commun.*, 2013, **49**, 11782–11784.
6 (*a*) G. Schiavon, G. Zotti, R. Toniolo and G. Bontempelli, *Anal. Chem.*, 1995, **67**, 318–323; (*b*) J. Doeller, T. Isbell, G. Benavides, J. Koenitzer, H. Patel, R. Patel, J. Lancaster, V. Darley-Usmar and D. Kraus, *Anal. Biochem.*, 2005, **341**, 40–51.
7 J. Furne, A. Saeed and M. D. Levitt, *Am. J. Physiol.*, 2008, **295**, R1479.
8 (*a*) W. Zheng, X. Lu, W. Wang, Z. Li, H. Zhang, Z. Wang, X. Xu, S. Li and C. Wang, *J. Colloid Interface Sci.*, 2009, **338**, 366–370; (*b*) L. Ji, A. Medford and X. Zhang, *Polymer*, 2009, **50**, 605–612; (*c*) L. Mai, L. Xu, Q. Gao, C. Han, B. Hu and Y. Pi, *Nano Lett.*, 2010, **10**, 2604–2608; (*d*) S. Mubeen, T. Zhang, N. Chartuprayoon, Y. Rheem, A. Mulchandani, N. Myung and M. Deshusses, *Anal. Chem.*, 2010, **82**, 250–257.
9 (*a*) J. Zhang, Y. Q. Sun, J. Liu, Y. Shi and W. Gou, *Chem. Commun.*, 2013, **49**, 11305–11307; (*b*) F. Yu, X. Han and L. Chen, *Chem. Commun.*, 2014, **50**, 12234–12249; (*c*) Z. Huang, S. Ding, D. Yu, F. Huang and G. Feng, *Chem. Commun.*, 2014, **50**, 9185–9187; (*d*) T. Ozdemir, F. Sozmen, S. Mamur, T. Tekinay and E. U. Akkaya, *Chem. Commun.*, 2014, **50**, 5455–5457; (*e*) Y. Zhou, J. Yu, X. Lei, J. Wu, Q. Niu, Y. Zhang, H. Liu, P. Christen, H. Gehringe and F. Wu, *Chem. Commun.*, 2013, **49**, 11782–11784.
10 (*a*) X. Zan and Z. Su, *Langmuir*, 2009, **25**, 12355–12360; (*b*) J. Wei, L. Wang, X. Zhang, X. Ma, H. Wang and Z. Su, *Langmuir*, 2013, **29**, 11413–11419; (*c*) X. Zan, M. Kozlov, T. McCarthy and Z. Su, *Biomacromolecules*, 2010, **11**, 1082–1088.
11 (*a*) C. Gu, H. Xu, M. Park and C. Shannon, *ECS Trans.*, 2008, **16**, 181–190; (*b*) C. Gu, H. Xu, M. Park and C. Shannon, *Langmuir*, 2009, **25**, 410–414.
12 J. Xu, X. Cui, J. Zhang, H. Liang, H. Wang and J. Li, *Bull. Mater. Sci.*, 2008, **31**, 189–192.
13 (*a*) A. Kryukov, A. Stroyuk, N. Zin'chuk, A. Korzhak and S. Kuchmii, *J. Mol. Catal. A: Chem.*, 2004, **221**, 209–221; (*b*) M. Pang, J. Hu and H. Zeng, *J. Am. Chem. Soc.*, 2010, **132**, 10771–10785.
14 M. Whiteman, S. Trionnaire, M. Chopra, B. Fox and J. Whatmore, *Clin. Sci.*, 2011, **121**, 459–488.